

Structure and dynamics of the proton within a light-front model

Emanuel Ydrefors

Institute of Modern Physics, China

Collaborators: T. Frederico and V. A. Karmanov and members from the BLFQ group

References: PRD 104, 114012 (2021), PRD 101, 096018 (2020), PLB 791, 276 (2019)

Light-Cone 2022: Physics of Hadrons on the Light Front
(Online)
Sep 20, 2022

- In hadron physics, one of the most important remaining challenges is to describe the dynamics and structure of the proton in terms of its basic constituents (quarks and gluons).
- The proton light-front wave function, defined on the null plane $x^+ = t + z = 0$, gives through the parton probability densities access to various observables.
- For example:
 - Electromagnetic form factors
 - The parton distribution function
 - Generalized parton distribution functions
- Additionally, the double parton scattering cross section depends on the double parton distribution function (DPDF) [1]:

$$D(x_1, x_2, \vec{\eta}_\perp) = \sum_{n=3}^{\infty} D_n(x_1, x_2, \vec{q}_\perp) = \sum_{n=3}^{\infty} \int \frac{d^2 k_{1\perp}}{(2\pi)^2} \frac{d^2 k_{2\perp}}{(2\pi)^2} \left\{ \prod_{i \neq 1,2} \int \frac{d^2 k_{i\perp}}{(2\pi)^2} \int_0^1 dx_i \right\} \times \delta\left(1 - \sum_{i=1}^n x_i\right) \delta\left(\sum_{i=1}^n \vec{k}_{i\perp}\right) \Psi_n^+(x_1, \vec{k}_{1\perp} + \vec{\eta}_\perp, x_2, \vec{k}_{2\perp} - \vec{\eta}_\perp, \dots) \Psi_n(x_1, \vec{k}_{1\perp}, x_2, \vec{k}_{2\perp}, \dots), \quad (1)$$

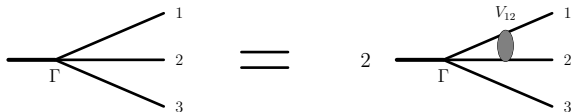
- The first of Mellin moments of DPDF has recently been calculated within lattice QCD [2].

[1] B. Blok et al, PRD 83 (2011) 071501 (R).

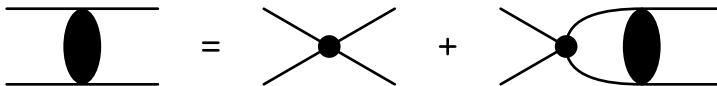
[2] G. S. Bali, JHEP09 (2021) 106.

- In the long-term perspective, to create a fully dynamical model for the proton in Minkowski space including the infinite number of Fock components in the state vector.
- It will then give direct access to observables defined on the light-front hyperplane.
- In that sense complementary to the BLFQ (Basis light-front Quantization) and the quark-diquark model by C. Roberts et al.
- As a first step, Fock basis truncated to valence order and spin degree-of-freedom not included.
- Quark-diquark model were the the quark-quark transition amplitude has a pole representing the s-wave diquark introduced through the zero-range interaction between two of the quarks. In that sense it is an effective low-energy model.
- The proton structure will be explored through the LF wave function and its Ioffe-time representation. Results for the momentum distributions will also be presented.

Three-body model



- Three spinless particles of mass m . Spectator + pair of interacting particles. Factor of two due to symmetry of wave function with respect to exchange of the particles.



- In the present work a zero-range interaction with four-leg-vertex $i\lambda$ used. Then, for the two-body amplitude (see figure)

$$i\mathcal{F}(M_{12}^2) = i\lambda + (i\lambda)^2\mathcal{B} + (i\lambda)^3\mathcal{B}^2 + \dots = \frac{1}{(i\lambda)^{-1} - \mathcal{B}(M_{12}^2)} \quad (2)$$

with

$$\mathcal{B}(M_{12}^2) = \int \frac{d^4k}{(2\pi)^4} \frac{i}{(k^2 - m^2 + i\epsilon)} \frac{i}{[(k-P)^2 - m^2 + i\epsilon]} \quad (3)$$

- Regularized and renormalized by fixing a diquark pole in the scattering amplitude.

- Faddeev-Bethe-Salpeter (FBS) equation with zero interaction [1]:

$$v(q, p) = 2i\mathcal{F}(M_{12}^2) \int \frac{d^4k}{(2\pi)^4} \frac{i}{k^2 - m^2 + i\epsilon} \frac{i}{(p - q - k)^2 - m^2 + i\epsilon} v(k, p) \quad (4)$$

- Currently, bare propagators for the quarks.
- $v(q, p)$ is one of the Faddeev components of the total vertex function.
- Di-quark concept introduced via assuming a pole in $\mathcal{F}(M_{12}^2)$, corresponding either to a two-body bound ($a > 0$) or virtual ($a < 0$) state, where a denotes the scattering length
- $\mathcal{F}(M_{12}^2)$, where $M_{12}^2 = (p - q)^2$, given by

$$\mathcal{F}(M_{12}^2) = \frac{\Theta(-M_{12}^2)}{16\pi^2 y \log \frac{1+y}{1-y} - \frac{1}{16\pi ma}} + \frac{\Theta(M_{12}^2) \Theta(4m^2 - M_{12}^2)}{8\pi^2 y' \arctan y' - \frac{1}{16\pi ma}} + \frac{\Theta(M_{12}^2 - 4m^2)}{16\pi^2 \log \frac{1+y''}{1-y''} - \frac{1}{16\pi ma} - \frac{iy''}{16\pi}}, \quad (5)$$

- The FBS equation was recently solved including the infinite number of Fock components in Euclidean [2] and Minkowski [3] space.

[1] T. Frederico, PLB 282 (1992) 409

[2] E. Ydrefors et al, PLB 770 (2017) 131

[3] E. Ydrefors et al, PLB 791 (2019) 276

Solution by direct integration of BS equation

- It is numerically challenging but possible to solve the three-body equation by direct integration.
- We used a similar approach as introduced by Carbonell and Karmanov [1] to solve the two-body problem (finite-range interaction).
- The equation for the vertex function, $v(q_0, q_v)$ can be written in the "non-singular" form

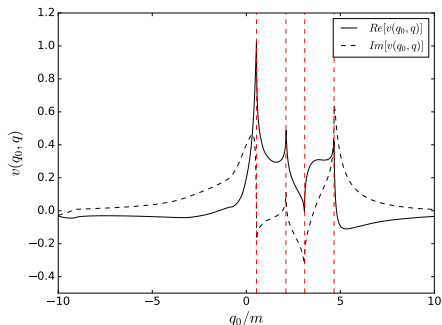
$$\begin{aligned} v(q_0, q_v) = & \frac{\mathcal{F}(M_{12}^2)}{(2\pi)^4} \int_0^\infty k_v^2 dk_v \left\{ i \frac{[\Pi(q_0, q_v; \varepsilon_k, k_v)v(\varepsilon_k, k_v) + \Pi(q_0, q_v; -\varepsilon_k, k_v)v(-\varepsilon_k, k_v)]}{2\varepsilon_k} \right. \\ & - 2 \int_{-\infty}^0 dk_0 \left[\frac{\Pi(q_0, q_v; k_0, k_v)v(k_0, k_v) - \Pi(q_0, q_v; -\varepsilon_k, k_v)v(-\varepsilon_k, k_v)}{k_0^2 - \varepsilon_k^2} \right] \\ & \left. - 2 \int_0^\infty dk_0 \left[\frac{\Pi(q_0, q_v; k_0, k_v)v(k_0, k_v) - \Pi(q_0, q; \varepsilon_k, k_v)v(\varepsilon_k, k_v)}{k_0^2 - \varepsilon_k^2} \right] \right\}, \end{aligned} \quad (6)$$

using, e.g, $[k_0^2 - k_v^2 - m^2 + i\epsilon]^{-1} = PV[k_0^2 - \varepsilon_k^2]^{-1} - i\pi/(2\varepsilon_k)[\delta(k_0 - \varepsilon_k) + \delta(k_0 + \varepsilon_k)]$. Above, where $\varepsilon_k = \sqrt{k_v^2 + m^2}$, $k_v = |\vec{k}|$ and the kernel Π only has weak, logarithmic, singularities. For $a < 0$ (considered here) $F(M_{12})$ has no pole.

- The singularities at $k_0 = \pm\varepsilon_k$ have been subtracted.

[1] J. Carbonell and V.A. Karmanov, PRD 90 (2014) 056002

Three-body vertex function in Minkowski space



- The figure shows the real and imaginary parts of $v(q_0, q_v)$ at fixed $q_v/m = 0.5$, for the case $a/m = -1.5$ and $B_3/m = 0.395$.
- The solution to the covariant equation has a quite non-smooth behavior. Namely:
- It is seen that there are four peaks (either singularities or branch cuts). It turns out that they have the positions $q_0 = M_3 \pm \sqrt{q_v^2 + 4m^2}$ and $q_0 = M_3 \pm q_v$, shown by red dashed lines. These are thus moving peaks depending on q_v .
- The non-smooth behavior of v makes the solution of this problem numerically very challenging.

- After the LF projection, i.e. introducing $k_{\pm} = k_0 \pm k_z$ and integrating over k_- , one obtains the three-body LF equation [1, 2]:

$$\Gamma(x, k_{\perp}) = \frac{\mathcal{F}(M_{12}^2)}{(2\pi)^3} \int_0^{1-x} \frac{dx'}{x'(1-x-x')} \int_0^{\infty} \frac{d^2 k'_{\perp}}{M_0^2 - M_N^2} \Lambda(M_0^2) \Gamma(x', k'_{\perp}) \quad (7)$$

with the squared free three-body mass

$$M_0^2 = (k_{\perp}^2 + m^2)/x' + (k_{\perp}^2 + m^2)/x + ((k'_{\perp} + k_{\perp})^2 + m^2)/(1-x-x') \quad (8)$$

- Form factor introduced via subtraction, i.e.

$$[M_0^2 - M_N^2]^{-1} - [M_0^2 + \mu^2]^{-1} = \Lambda(M_0^2)[M_0^2 - M_N^2]^{-1} \rightarrow \Lambda(M_0^2) = [M_0^2 + \mu^2]^{-1}[M_N + \mu^2], \quad (9)$$

where μ is a cut-off mass.

- The form factor eliminates the unphysical ground state, with $M_N^2 < 0$, and also lead to an infrared enhancement.
- The three-body valence LF wave function is given by

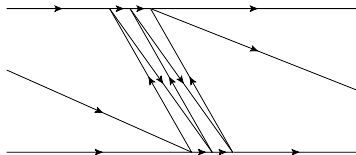
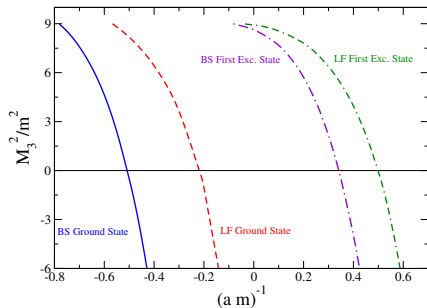
$$\Psi_3(x_1, \vec{k}_{1\perp}, x_2, \vec{k}_{2\perp}, x_3, \vec{k}_{3\perp}) = \frac{\Gamma(x_1, \vec{k}_{1\perp}) + \Gamma(x_2, \vec{k}_{2\perp}) + \Gamma(x_3, \vec{k}_{3\perp})}{\sqrt{x_1 x_2 x_3} (M_N^2 - M_0^2(x_1, \vec{k}_{1\perp}, x_2, \vec{k}_{2\perp}, x_3, \vec{k}_{3\perp}))}, \quad (10)$$

where due to momentum conservation: $x_3 = 1 - x_2 - x_1$ and $\vec{k}_{3\perp} = -\vec{k}_{1\perp} - \vec{k}_{2\perp}$.

[1] J. Carbonell and V.A. Karmanov, PRC 67 (2003) 037001

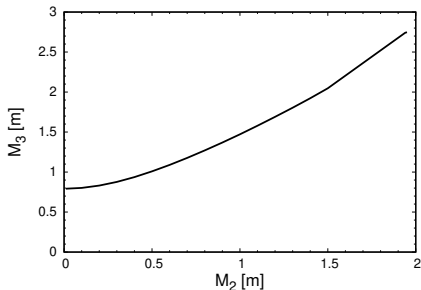
[2] T. Frederico, PLB 282 (1992) 409

Binding energy versus inverse scattering length (BS vs LF) $\Lambda = 1$



- The (complete) BS equation gives a stronger bound system compared to the LF one for all a .
- Exists a region with $a < 0$ (i.e. a Borromean system) the solution with the smallest M_3^2 , i.e. the formal ground state, is physical.
- However, for $a > 0$, i.e. a two-body bound state exists, the lowest state is unphysical.
- $M_3^2 > -\infty$: No Thomas collapse in the non-relativistic sense, i.e. an effective short-range repulsion.
- The higher-Fock state contributions beyond the valence to the kernel can be interpreted as an effective three-body force of relativistic origin.

Computed binding energy including form factor



- Three-body mass v.s. di-quark mass for the ground state using $\mu = 3m$.
- It is known that the spurious state has become physical for the full range of M_2 .
- With increasing μ the M_3 decreases and becomes then imaginary, i.e. the spurious g.s. state appears.

- The valence contribution to the Dirac form factor is given by (using the + part of the EM current)

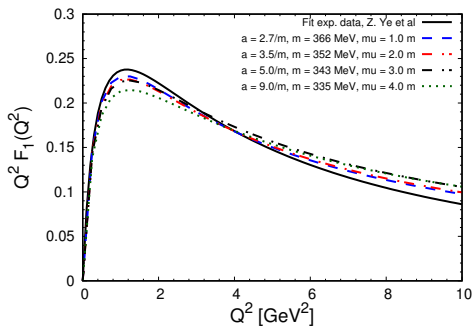
$$F_1(Q^2) = \left\{ \prod_{i=1}^3 \int \frac{d^2 k_{i\perp}}{(2\pi)^2} \int_0^1 dx_i \right\} \delta \left(1 - \sum_{i=1}^3 x_i \right) \delta \left(\sum_{i=1}^3 \vec{k}_{i\perp}^f \right) \Psi_3^\dagger(x_1, \vec{k}_{1\perp}^f, \dots) \Psi_3(x_1, \vec{k}_{1\perp}^i, \dots), \quad (11)$$

where $Q^2 = \vec{q}_\perp \cdot \vec{q}_\perp$ and the magnitudes of the momenta read

$$|\vec{k}_{i\perp}^{f(i)}|^2 = |\vec{k}_{i\perp} \pm \frac{\vec{q}_\perp}{2} x_i|^2 = \vec{k}_{i\perp}^2 + \frac{Q^2}{4} x_i^2 \pm \vec{k}_{i\perp} \cdot \vec{q}_\perp x_i \quad (i = 1, 2), \quad (12)$$

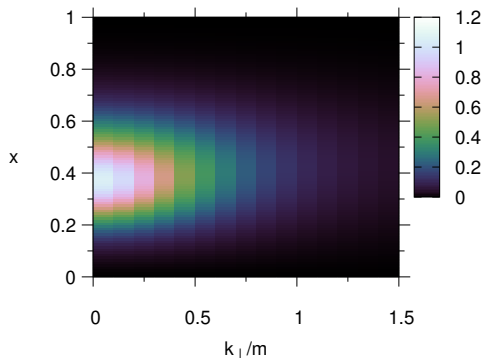
and

$$\begin{aligned} |\vec{k}_{3\perp}^{f(i)}|^2 &= \left| \pm \frac{\vec{q}_\perp}{2} (x_3 - 1) - \vec{k}_{1\perp} - \vec{k}_{2\perp} \right|^2 = \\ &= (1 - x_3)^2 \frac{Q^2}{4} \pm (1 - x_3) \vec{q}_\perp \cdot (\vec{k}_{1\perp} + \vec{k}_{2\perp}) + (\vec{k}_{1\perp} + \vec{k}_{2\perp})^2. \end{aligned} \quad (13)$$

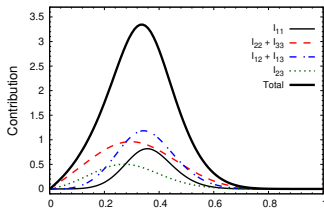


- In figure $Q^2 F_1(Q^2)$ for different values of a and μ compared with fit to exp. data by Z. Ye et al.
- Best agreement obtained for $a = 2.7/m$ and $\mu = m$ with a constituent quark mass $m = 366$ MeV, and this parameters will be used in the following.
- Fair agreement with exp. data for $Q^2 < 5 \text{ GeV}^2$ but for larger values of Q^2 they deviate, presumably due to lack of a finite-range interaction.

Results for the vertex function



- The proton structure contained in the vertex function $\Gamma(x, k_{\perp})$. Concentrated at small k_{\perp} and $x \sim 1/3$. Expected since we have a bound state of a three-particle system.



- The single parton distribution function (PDF), is the integrand of the form factor at $Q^2 = 0$, i.e.

$$f_1(x_1) = \frac{1}{(2\pi)^6} \int_0^{1-x_1} dx_2 \int d^2k_{1\perp} d^2k_{2\perp} |\Psi_3(x_1, \vec{k}_{1\perp}, x_2, \vec{k}_{2\perp}, x_3, \vec{k}_{3\perp})|^2 = I_{11} + I_{22} + I_{33} + I_{12} + I_{13} + I_{23}. \quad (14)$$

with the Faddeev contributions

$$I_{ii} = \frac{1}{(2\pi)^6} \int_0^{1-x_1} dx_2 \int d^2k_{1\perp} d^2k_{2\perp} \frac{\Gamma^2(x_i, \vec{k}_{i\perp})}{x_1 x_2 x_3 (M_N^2 - M_0^2(x_1, \vec{k}_{1\perp}, x_2, \vec{k}_{2\perp}, x_3, \vec{k}_{3\perp}))^2} \quad (15)$$

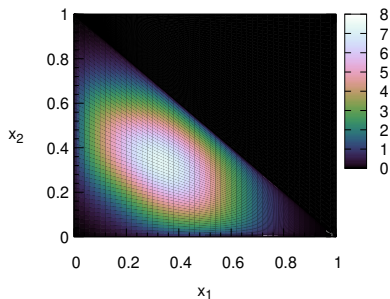
$$I_{ij} = \frac{2}{(2\pi)^6} \int_0^{1-x_1} dx_2 \int d^2k_{1\perp} d^2k_{2\perp} \frac{\Gamma(x_i, \vec{k}_{i\perp}) \Gamma(x_j, \vec{k}_{j\perp})}{x_1 x_2 x_3 (M_N^2 - M_0^2(x_1, \vec{k}_{1\perp}, x_2, \vec{k}_{2\perp}, x_3, \vec{k}_{3\perp}))^2}; \quad i \neq j.$$

- The PDF at model scale is peaked around $x = 1/3$ and quite narrow. None of the Faddeev contributions are negligible.

- For the comparison with other frameworks and/or experimental data the PDF should be evolved from the model scale to a higher scale.
- In this work we use the all-order DGLAP evolution (see e.g. talk by Craig) and the process-independent charge (EPJC 80 (2020) 1064):

$$\alpha(k^2) = \frac{\gamma_m \pi}{\log[\mathcal{K}^2(k^2)/\Lambda_{\text{QCD}}^2]}, \quad \mathcal{K}^2(y) = (a_0^2 + a_1 y + y^2)/(b_0 + y) \quad (16)$$

- The initial scale is given by the hadron scale $Q_0 = 0.330 \pm 0.03$ GeV.
- The same evolution framework was used successfully for the pion (see previous talk by W. de Paula).



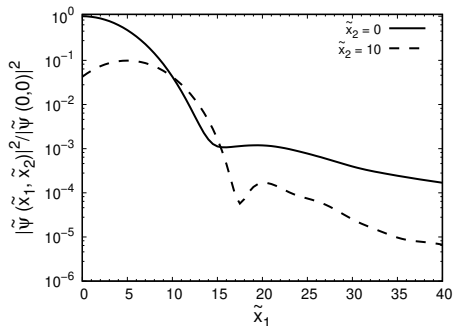
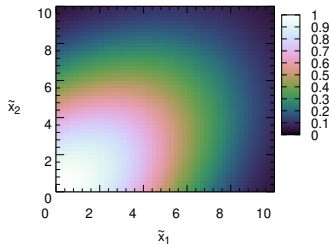
- The distribution amplitude is defined as

$$\phi(x_1, x_2) = \int d^2k_{1\perp} d^2k_{2\perp} \Psi_3(x_1, \vec{k}_{1\perp}, x_2, \vec{k}_{2\perp}, x_3, \vec{k}_{3\perp}). \quad (17)$$

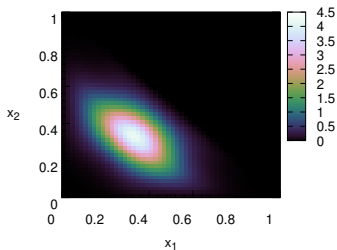
- It shows the dependence of the wave function on the momentum fractions for the case when the quarks share the same position.
- Triangular shape due to $x_1 + x_2 \leq 1$. Distribution centered around $x_1 = x_2 = 1/3$ but quite wide.

- Alternatively, the proton can be studied in the on the null-plane, in terms of the transverse position ($\vec{b}_{i\perp}$) and the Ioffe-time $\tilde{x}_i = b_i^- p^+$. The image of the proton is then obtained through the Fourier transform of the proton LF wave function.
- For simplicity, we consider here the case $\vec{b}_{1\perp} = \vec{b}_{2\perp} = \vec{0}_\perp$, and then one has

$$\Phi(\tilde{x}_1, \tilde{x}_2) \equiv \tilde{\Psi}_3(\tilde{x}_1, \vec{0}_\perp, \tilde{x}_2, \vec{0}_\perp) = \int_0^1 dx_1 e^{i\tilde{x}_1 x_1} \int_0^{1-x_1} dx_2 e^{i\tilde{x}_2 x_2} \phi(x_1, x_2), \quad (18)$$



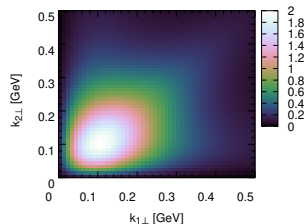
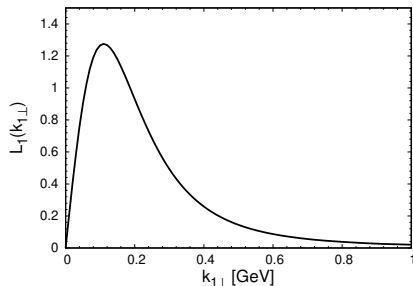
- For $\tilde{x}_1 \geq 10$ a rather dramatic decrease of the amplitude is seen.
- An exponential damping is seen with respect to the relative distance in Ioffe-time between the two quarks. We expect this damping to be even more significant if confinement is incorporated, as its more effective at large distances.



- The valence double parton distribution function (DPDF) is given by

$$D_3(x_1, x_2; \vec{\eta}_\perp) = \frac{1}{(2\pi)^6} \int d^2k_{1\perp} d^2k_{2\perp} \times \Psi_3^\dagger(x_1, \vec{k}_{1\perp} + \vec{\eta}_\perp; x_2, \vec{k}_{2\perp} - \vec{\eta}_\perp; x_3, \vec{k}_{3\perp}) \Psi_3(x_1, \vec{k}_{1\perp}; x_2, \vec{k}_{2\perp}; x_3, \vec{k}_{3\perp}). \quad (19)$$

- Fourier transform of $D_3(x_1, x_2, \vec{\eta}_\perp)$ in $\vec{\eta}_\perp$ gives the probability of finding the quarks 1 and 2 with momentum fractions x_1 and x_2 at a relative distance \vec{y}_\perp within the proton.
- In the figure is shown results for $\eta_\perp = 0$, showing a distribution centered around $x_1 = x_2 = 1/3$.



- The single quark transverse momentum density in the forward limit and integrated in the longitudinal momentum is associated with the probability density to find a quark with momentum k_{\perp} .
- It can be computed as:

$$L_1(k_{1\perp}) = \frac{k_{1\perp}}{(2\pi)^6} \int_0^1 dx_1 \int_0^{1-x_1} dx_2 \int_0^{2\pi} d\theta_1 \int d^2k_{2\perp} |\psi_3(x_1, \vec{k}_{1\perp}, x_2, \vec{k}_{2\perp}, x_3, \vec{k}_{3\perp})|^2. \quad (20)$$

- Two-quark one:

$$L_2(k_{1\perp}, k_{2\perp}) = \frac{k_{1\perp} k_{2\perp}}{(2\pi)^6} \int_0^1 dx_1 \int_0^{1-x_1} dx_2 \int_0^{2\pi} d\theta_1 \int_0^{2\pi} d\theta_2 |\psi_3(x_1, \vec{k}_{1\perp}, x_2, \vec{k}_{2\perp}, x_3, \vec{k}_{3\perp})|^2. \quad (21)$$

- The three-body FBS equation with zero-range interaction, including the infinite number of Fock components, was solved by direct integration in Minkowski space in Ref. [1]. However, the solution was quite difficult from numerical point of view.
- However, like in the two-body case, the Nakanishi integral representation be used for vertex function:

$$v(q;p) = \int_{-4/3}^{2/3} dz \int_0^\infty \frac{d\gamma g(\gamma, z)}{\gamma - k^2 - (p \cdot q)z - i\epsilon} \quad (22)$$

- For the two-body scattering amplitude

$$\mathcal{F}(M_{12}^2) = \int_{4m^2}^\infty d\gamma \frac{\rho(\gamma)}{M_{12}^2 - \gamma + i\epsilon} \quad (23)$$

with the spectral function

$$\rho(\gamma) = -\frac{\theta(s - 4m^2)}{16\pi^2} \frac{y''}{\left(\frac{y''}{16\pi^2} \log \frac{1+y''}{1-y''} - \frac{1}{16\pi m a}\right)^2 + \left(\frac{y''}{16\pi}\right)^2} \quad (24)$$

- Construction of the integral equation for $g(\gamma, z)$ and its solution is under development.
- Observables could then be computed including all the infinite number of Fock components.

[1] E. Ydrefors et al, PLB 791 (2019) 276

By assuming the uniqueness of the Nakanishi weight function one can derive the following equation for $g(\gamma, z)$:

$$g(\gamma, z) = -\frac{2}{(4\pi)^2(z + \frac{4}{3})^4} \int_{-\frac{4}{3}}^{\frac{2}{3}} dz' \left(\frac{2}{3} - z'\right)^2 \theta\left(\left(\frac{2}{3} - z'\right) - \left(z + \frac{4}{3}\right)\right) \int_{4m^2}^1 \rho(\gamma'') d\gamma'' \int_{\frac{z+\frac{4}{3}}{\frac{2}{3}-z'}}^1 \frac{d\alpha_1}{\alpha_1} \int_0^{\frac{z+\frac{4}{3}}{\frac{2}{3}-z'}} d\alpha_3 \left[\left(z + \frac{4}{3}\right) - \alpha_3 \left(\frac{2}{3} - z'\right) \right] \frac{\partial g(\gamma_0, z')}{\partial \gamma_0} \theta(\gamma_0) \quad (25)$$

where

$$\gamma_0 = \frac{p^2}{9} + m^2 - z' \frac{p^2}{3} - \frac{1}{4} \frac{\alpha_3}{\alpha_1} \left(\frac{2}{3} - z'\right)^2 p^2 - \frac{\alpha_1}{\alpha_3} m^2 + \frac{(\frac{2}{3} - z')}{(z + \frac{4}{3})^2} \times \left[\left(z + \frac{4}{3}\right) - \alpha_3 \left(\frac{2}{3} - z'\right) \right] \left[\gamma - (1 - \alpha_1) \gamma'' - \frac{2}{3} p^2 \left(\frac{2}{3} + z\right) \right]. \quad (26)$$

The numerical solution of this equation will be attempted in the near future.

- We have, in this work, studied the proton in a simple but fully dynamical valence LF model based on a zero-range interaction.
- The model is based on the concept of a strongly interacting scalar diquark.
- We have studied the structure of the proton by computing the LF wave function in its Ioffe-time representation and also momentum distributions.
- However, the model is rather crude since e.g. the spin degree of freedom hasn't been included yet. But is a first step towards studying the proton directly in Minkowski space.
- Future plans:
 - Generalization to the infinite set of Fock components (The Faddeev-Bethe-Salpeter equation solved in PLB 791 (2019) 276)
 - Implementation of a more realistic interaction (gluon exchange)
 - Inclusion of spin degree of freedom